第 32 卷第 5 期
2016 年 5 月

无 机 化 学 学 报
CHINESE JOURNAL OF INORGANIC CHEMISTRY

Vol.32 No.5
753-761

3,6-二(*N*-咪唑/苯并咪唑基)哒嗪配体配合物的合成、结构、荧光及光催化性能

李金萍　范建中　王多志*

(新疆大学化学化工学院,乌鲁木齐　830046)

摘要：用溶剂热法设计、合成了 4 个金属–有机配合物 $[Mn(L^1)_4(OH)_2]$ (**1**), $\{[MnL^1(H_2O)_4]SO_4\}_n$ (**2**), $[CdL^2(NO_3)_2]_n$ (**3**)和 $\{[Co(L^2)_2](PF_6)_2\}_n$ (**4**), (L^1=3,6-二(*N*-咪唑基)哒嗪, L^2=3,6-二(*N*-苯并咪唑基)哒嗪),并通过元素分析、红外、X 射线单晶衍射对配合物结构进行了表征,测试结果表明配合物 **1** 具有单核结构,**2** 为一维链结构,配合物 **3** 和 **4** 均为二维网状结构。此外,对配合物 **3** 和 **4** 的固态荧光性能及光催化的性能做了进一步研究。

关键词：配合物；晶体结构；荧光性能。
中图分类号：O614.71+1；O614.24+2 O614.81+2　　**文献标识码**：A　　**文章编号**：1001-4861(2016)05-0753-09
DOI:10.11862/CJIC.2016.093

Metal-Organic Complexes Based on 3,6-Bis(*N*-imidazolyl/benzimidazolyl) Pyridazine: Syntheses, Structures, Emission and Photocatalytic Properties

LI Jin-Ping　FAN Jian-Zhong　WANG Duo-Zhi*

(*College of Chemistry and Chemical Engineering, Xinjiang University, Urumqi* 830046, *China*)

Abstract: Four new metal-organic coordination polymers namely, $[Mn(L^1)_4(OH)_2]$ (**1**), $\{[MnL^1(H_2O)_4](SO_4)\}_n$ (**2**), $[CdL^2(NO_3)_2]_n$ (**3**), $\{[Co(L^2)_2](PF_6)_2\}_n$ (**4**) (L^1=3,6-bis(*N*-imidazolyl) pyridazine, L^2=3,6-bis(*N*-benzimidazolyl) pyridazine] have been synthesized under solvothermal conditions and characterized by elemental analyses, IR spectra as well as single-crystal X-ray diffraction analysis. The analysis reveals that complex **1** has a mononuclear structure, and complex **2** features a 1D structure. Complexes **3** and **4** exhibit 2D network structures. The fluorescence and photocatalytic activities of the complexes **3** and **4** have been investigated and discussed. CCDC: 1444988, **1**; 1444989, **2**; 1022876, **3**; 1022877, **4**.

Keywords: complex; crystal structure; luminescent property

0 Introduction

In the past decades, a growing interest in the study of metal-organic coordination polymers (MOFs) has attracted much attention owing to their various structural and potential applications in the area of catalysis, fluorescence, chemical sensors, ion exchange, gas storage[1-5]. For the construction of metal-organic coordination polymers, the most critical strategy is the rational design and selection of the appropriate ligands, which possess versatile coordination modes and strong coordination abilities to metal ions[6-8]. Up to now, a great number of MOFs with various structures such as zero-dimensional (0D)

收稿日期:2016-01-05。收修改稿日期:2016-03-01。
国家自然科学基金(No.21361026)资助项目。
*通信联系人。E-mail:wangdz@xju.edu.cn;会员登记号:S06N9862M1207。

clusters[9], 1D chains[10], 2D layers[11] and 3D frameworks[12] have been reported. At the same time, to analysis topology of MOFs is not only an effective tool for simplifying the complicated structures but also play an important role in the deliberate design of certain MOFs with specific properties[13]. However, it is still a great challenge to construct target coordination polymers with desired structures and functional properties[14].

So far, humanity is faced with serious environmental pollution including atmospheric pollution, soil pollution, water pollution and so on. The most serious is the water pollution, which not only could poison creatures living in the water but also damage people′s health. Considerable efforts have been made in treating waste water with many methods such as adsorption and separation, chemical treatment, photocatalysis[15]. In addition, MOFs have attracted much attention because of their photocatalysis properties in purifying waste water by thoroughly decomposing organic pollutants[16]. This is a convenient and recyclable approach to solve the problem of water pollution.

In recent years, a series of N-containing heterocyclic ligands containing bis (imidazolyl/benzimidazolyl) have attracted much attention owing to their remarkable features as follows: (a) The ligands have an identical ring size and a similar set of donor atoms[17]. (b) They contain two imidazole rings, which nitrogen atoms can act as hydrogen bond donors to build hydrogen bond interaction and their rings can form π-π stacking interaction[18]. (c) They exhibit a wide variety of pharmacological activities like fungicides or anti-helminthics[19]. Therefore, a large number of metal coordination compounds with bis (imidazolyl/benzimidazolyl) about luminescent properties and photocatalytic activity for (methylene blue) MB dye degradation have been reported[20].

In this work, we carried out research on the coordination chemistry of pyridazine containing ligand. We designed and synthesized ligands 3,6-bis (*N*-imidazolyl) pyridazine (L^1) and 3,6-bis (*N*-benzimidazolyl) pyridazine (L^2) (Chart 1) and successfully prepared four novel complexes, namely, $[Mn(L^1)_4(OH)_2]$ (**1**), $\{[MnL^1(H_2O)_4]SO_4\}_n$ (**2**), $[CdL^2(NO_3)_2]_n$ (**3**), $\{[Co(L^2)_2](PF_6)_2\}_n$ (**4**). We also discuss the syntheses, crystal structures of complexes **1**~**4** and analysis the topology of complex **4**. Furthermore, the luminescent properties and photocatalytic activities of the complexes **3** and **4** have been investigated and discussed.

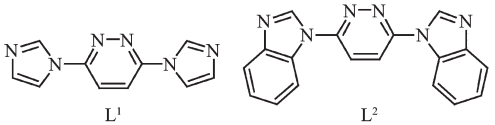

L^1 L^2

Chart 1 Structures of the ligands L^1 and L^2

1 Experimental

1.1 Materials and general methods

All reagents were purchased commercially and used without further purification. Elemental analyses (C, H, N) were performed on a Thermo Flash EA 1112-NCHS-O analyzer. IR spectra were measured on a Brucker Equinox 55 FT-IR spectrometer with KBr Pellets in the range of 4 000~400 cm^{-1}. ^1H NMR data were collected using an INOVA-400 NMR spectrometer. TGA of complexes **1** and **2** were performed on a DSC200F3 analyzer heated from 30 to 1 000 ℃, and TGA of complexes **3** and **4** were performed on a Perkin-Elmer TG-7 analyzer heated from 30 to 700 ℃. The X-ray powder diffraction patterns (XRPD) of **1**~**4** were recorded on a Bruker D8 automated diffractometer, operated at 40 kV and 100 mA, using a Cu-target tube and a graphite monochromator ($K\alpha$ radiation, λ=0.154 18 nm). Fluorescence spectra were performed using a Hitachi F-4500 Fluorescence Spectrophotometer with a Xe arc lamp as the light source and bandwidths of 2.5 nm at room temperature. UV-Vis absorption spectra were obtained using a Hitachi UV-3010 UV-Vis spectrophotometer.

1.2 Synthesis of ligand L^1

Imidazole (3.4 g, 49.9 mmol), sodium (1.2 g, 52.2 mmol) and 80 mL THF was added to a 250 mL three-necked flask. The reaction mixture was refluxed for 40 min. A solution of 3,6-dichloropyridazine (3.7 g, 24.8 mmol) in 10 mL THF was added to the mixture within 40 min. The mixture was refluxed for 4 h under N_2. The reaction mixture was poured into ice

water after cooled to room temperature. The earthy yellow solid of L^1 was obtained after filtering. Pure ligand L^1 was obtained by recrystallization from ethanol as white crystals. Yield: 80%. m.p. 281~282 ℃. ^{1}H NMR (DMSO-d_6): δ 8.69 (s, 2H, imidazole-2), 8.58 (s, 2H, pyridazine), 8.11 (s, 2H, imidazole-5), 7.23 (s, 2H, imidazole-4); Anal. Calcd. for $C_{10}H_8N_6$ (%): C, 56.60; H, 3.79; N, 39.60; Found (%): C, 56.75; H, 3.75; N, 39.54. IR (KBr, cm^{-1}): 3 145 (m), 3 109 (m), 3 047 (m), 3 018 (m), 1 645 (w), 1 577 (s), 1 519 (s), 1 490 (s), 1 459 (s), 1 371 (m), 1 321 (s), 1 277 (m), 1 237 (m), 1 163 (m), 1 106 (m), 1 059 (m), 1 031 (s), 962 (m), 903 (m), 861 (s), 823 (s), 766 (s), 749 (s), 645 (s), 613 (m), 507 (w), 487 (m).

1.3 Synthesis of ligand L^2

Ligand L^2 was synthesized similarly as L^1 by using benzimidazole instead of imidazole. Yield: 76%. m.p. 283~284 ℃. ^{1}H NMR (DMSO-d_6): δ 9.130 (s, 2H, imidazole-2), 8.653 (s, 2H, pyridazine), 7.388~8.384 (m, 8H, benzene); Anal. Calcd. for $C_{18}H_{12}N_6$ (%): C, 69.21; H, 3.87; N, 26.91; Found (%): C, 69.34; H, 3.56; N, 27.41. IR (KBr, cm^{-1}): 3 082 (m), 3 058 (m), 1 669 (w), 1 609 (m), 1 590 (m), 1 558 (s), 1 497 (s), 1 459 (s), 1 359 (m), 1 338 (m), 1 308 (m), 1 279 (m), 1 238 (m), 1 190 (s), 1 163 (m), 1 138 (m), 1 035 (m), 979 (m), 939 (m), 884 (m), 830 (m), 769 (s), 753 (s), 732 (s), 623 (m), 575 (m), 486 (m), 427 (m).

1.4 Synthesis of complex 1

A mixture of $Mn(BF_4)_2\cdot 4H_2O$ (90 mg, 0.3 mmol), L^1 (63 mg, 0.3 mmol) and 5 mL water was sealed in a 25 mL Teflon-lined stainless steel vessel and heated at 140 ℃ for 48 h, then cooled to room temperature at a rate of 10 ℃·h^{-1}. The colorless block crystals were obtained (*ca.* 36% yield based on L^1). Anal. Calcd. for $C_{40}H_{34}MnN_{24}O_2$(%): C, 51.22; H, 3.65; N, 35.84. Found (%): C, 52.48; H, 3.97; N, 36.76. IR (KBr, cm^{-1}): 3 600 (m), 3 387 (m), 3 119 (m), 1 580 (m), 1 522 (s), 1 481 (s), 1 319 (s), 1 242 (m), 1 098 (m), 1 064 (s), 1 033 (s), 968 (m), 918 (m), 838 (m), 738 (m), 651 (m), 615 (m), 492 (m).

1.5 Synthesis of complex 2

2 was synthesized similarly as **1** by using $MnSO_4\cdot H_2O$ instead of $Mn(BF_4)_2\cdot 4H_2O$. The colorless block crystals were obtained (*ca.* 36% yield based on L^1). Anal. Calcd. for $C_{10}H_{16}MnN_6O_8S$ (%): C, 27.59; H, 3.70; N, 19.30. Found (%): C, 27.43; H, 3.89; N, 19.57. IR (KBr, cm^{-1}): 3 167 (m), 3 130 (m), 1 643 (m), 1 581 (m), 1 495 (s), 1 456 (s), 1 303 (s), 1 258 (m), 1 073 (s), 1 044 (s), 966 (m), 924 (m), 823 (m), 773 (m), 728 (m), 643 (m), 616 (m), 597 (m), 494 (m).

1.6 Synthesis of complex 3

A mixture of $Cd(NO_3)_2\cdot 4H_2O$ (30 mg, 0.1 mmol), L^2 (31 mg, 0.1 mmol) and 5 mL methanol was sealed in a 25 mL Teflon-lined stainless steel vessel and heated at 140 ℃ for 48 h, then cooled to room temperature at a rate of 10 ℃·h^{-1}. The colorless block crystals were obtained (*ca.* 36% yield based on L^2). Anal. Calcd. for $C_{18}H_{12}CdN_8O_6$ (%): C, 39.39; H, 2.20; N, 20.41. Found (%): C, 40.48; H, 2.88; N, 23.74. IR (KBr, cm^{-1}): 3 116 (m), 3 104 (m), 3 050 (m), 1 611 (m), 1 584 (m), 1 562 (m), 1 504 (s), 1 462 (s), 1 442 (s), 1 399 (m), 1 378 (m), 1 349 (m), 1 322 (s), 1 298 (s), 1 248 (s), 1 232 (s), 1 044 (m), 1 037 (m), 1 013 (m), 909 (m), 884 (m), 855 (m), 808(m), 703 (m), 739 (s), 619 (m).

1.7 Synthesis of complex 4

4 was synthesized similarly as **3** by using $Co(PF_6)_2\cdot 6H_2O$ (46 mg, 0.1 mmol) instead of $Cd(NO_3)_2\cdot 4H_2O$. The purple block crystals were obtained (*ca.* 45% yield based on L^2). Anal. Calcd. for $C_{36}H_{24}CoF_{12}N_{12}P_2$ (%): C, 44.41; H, 2.48; N, 17.26. Found(%): C, 45.02; H, 2.56; N, 18.37. IR (KBr, cm^{-1}): 3 147 (w), 3 073 (w), 1 569 (m), 1 504 (s), 1 465 (s), 1 439 (s), 1 298 (m), 1 232 (s), 1 156 (m), 1 092 (s), 1 042 (m), 1 014 (m), 915 (m), 837 (m), 780 (m), 748 (s), 612 (m), 448 (m), 417 (m).

1.8 Determination of photocatalytic activity

50 mg of complexes **3** and **4** were mixed together with 50 mL of an aqueous solution of MB (10 mg·L^{-1}). Then the solution was exposed to UV irradiation under an Hg lamp (300 W) for 4 h and kept stirring during irradiation. Samples of 5 mL were taken away every 30 min for UV measurement.

1.9 Structure determination

Experimental reflections were collected with a Bruker APEX Ⅱ Smart CCD diffractometer using

Mo $K\alpha$ radiation (λ=0.071 073 nm) (Table 1). The program SAINT[21] was used for integration of the diffraction profiles. The structures of **1~4** were solved by the direct method and refined by the full-matrix least squares on F^2 using the SHELXTL[22a]. Semi-empirical absorption corrections were carried out using SADABS[22b] program. Hydrogen atoms of carbon were located at calculated positions and refined with fixed thermal parameters riding on their parent atoms. All non-hydrogen atoms were refined with anisotropic displacement parameters. The complex **4** exhibited a structure disorder. Experimental details for the structure determination are presented in Table 1. The selected bond distances and angles were listed in Table 2.

CCDC: 1444988, **1**; 1444989, **2**; 1022876, **3**; 1022877, **4**.

Table 1 Crystallographic data for complexes 1~4

Complex	1	2	3	4
Empirical formula	$C_{40}H_{34}N_{24}MnO_2$	$C_{10}H_{16}MnN_6O_8S$	$C_{18}H_{12}CdN_8O_6$	$C_{36}H_{24}CoF_{12}N_{12}P_2$
Formula weight	937.85	435.29	548.77	973.54
Crystal system	Monoclinic	Tetragonal	Monoclinic	Tetragonal
Space group	*Pc*	$P4_12_12$	$P2_1/c$	$P4_2/n$
T / K	293(2)	296(2)	293(2)	296(2)
a / nm	1.556 1(4)	0.927 67(3)	0.521 98(8)	1.264 54(4)
b / nm	1.391 8(4)	0.927 67(3)	1.188 65(18)	1.264 54(4)
c / nm	1.392 5(4)	3.671 4(2)	3.129 9(4)	1.128 37(5)
β / (°)	114.245(6)		98.107(3)	
V / nm^3	2.749 8(13)	3.159 5(2)	1.922 5(5)	1.804 33
Z	2	8	4	2
D_c / ($g\cdot cm^{-3}$)	1.133	1.830	1.896	1.792
Absorption coefficient / mm^{-1}	0.294	1.027	1.196	0.677
F(000)	966	1 784	1 088	978
Reflections collected	17 390	8 195	10 475	11 196
Unique (R_{int})	7 717 (0.069 5)	2 313 (0.043 8)	3 358 (0.053 7)	1 587 (0.033 4)
Goodness-of-fit on F^2	1.055	1.042	1.064	1.034
Data, restraints, parameters	7 717, 4, 609	2 313, 24, 259	3 358, 0, 298	1 587, 69, 163
Final *R* indices[a,b] [$I>2\sigma(I)$]	R_1=0.078 8, wR_2=0.256 6	R_1=0.066 1, wR_2=0.169 8	R_1=0.042 6, wR_2=0.093 3	R_1=0.056 5, wR_2=0.271 0
R indices[a,b] (all data)	R_1=0.135 6, wR_2=0.283 3	R_1=0.075 9, wR_2=0.175 5	R_1=0.048 9, wR_2=0.095 2	R_1=0.108 4, wR_2=0.283 2

[a] $R_1=\sum(||F_o|-|F_c||)/\sum|F_o|$; [b] $wR_2=[\sum w(|F_o|^2-|F_c|^2)^2/\sum w(F_o^2)]^{1/2}$

Table 2 Selected bond distances (nm) and angles (°) for complexes 1~4

1					
Mn1-O1	0.214 9(5)	Mn1-O2	0.216 5(5)	Mn1-N6	0.222 8(7)
Mn1-N7	0.225 3(6)	Mn1-N13	0.226 3(7)	Mn1-N19	0.225 4(7)
O1-Mn1-N6	94.3(3)	O2-Mn1-N6	86.2(3)	O1-Mn1-N7	86.2(2)
O2-Mn1-N7	94.6(3)	N6-Mn1-N7	92.9(3)	O1-Mn1-N19	87.0(2)
O2-Mn1-N19	92.3(3)	N19-Mn1-N13	93.1(3)	N6-Mn1-N19	87.4(3)
O2-Mn1-N13	85.6(3)	N7-Mn1-N13	87.6(3)	O1-Mn1-N13	94.0(3)

Continued Table 2

			2		
Mn1-O4	0.216 5(5)	Mn1-O1	0.218 4(5)	Mn1-O2	0.219 9(5)
Mn1-O3	0.222(5)	Mn1-N1^{i}	0.226 2(5)	Mn1-N6	0.226 1(5)
O4-Mn1-O2	83.2(2)	O1-Mn1-O2	86.2(2)	O4-Mn1-O3	83.5(2)
O1-Mn1-O3	86.5(2)	O2-Mn1-O3	87.9(2)	O4-Mn1-N1^{i}	95.8(2)
O1-Mn1-N1^{i}	93.9(2)	O3-Mn1-N1^{i}	86.89(19)	O4-Mn1-N6	95.3(3)
O1-Mn1-N6	93.7(2)	O2-Mn1-N6	86.7(2)	N1^{i}-Mn1-N6	98.6(2)
			3		
Cd1-N3	0.225 2(4)	Cd1-N2	0.226 3(4)	Cd1-O4	0.230 8(4)
Cd1-O3	0.235 9(3)	Cd1-O2^{ii}	0.244 6(3)	Cd1-O1	0.271 4(3)
Cd1-O6	0.282 5(5)				
N3-Cd1-N2	105.01(14)	N3-Cd1-O4	90.20(15)	N2-Cd1-O3	86.78(12)
O4-Cd1-O3	84.11(13)	N2-Cd1-O2^{ii}	92.32(13)	O3-Cd1-O2$_{ii}$	78.96(11)
O4-Cd1-O2^{ii}	72.09(12)	N3-Cd1-O4	90.20(15)	N3-Cd1-O1	101.22(12)
O1-Cd1-O6	60.96(11)	N2-Cd1-O1	79.25(12)	O3-Cd1-O1	49.95(10)
N3-Cd1-O6	81.85(16)	O4-Cd1-O6	47.98(12)	O3-Cd1-O6	70.21(14)
			4		
Co1-N1	0.199 6(5)				
N1^{ii}-Co1-N1^{iii}	112.8(3)	N1ii-Co1-N1	107.84(14)		

Symmetry codes: ^{i} $x-1$, $y-1$, z for **2**; ^{ii} $-y+1/2$, x, $-z+1/2$ for **3**; ^{ii} $-y+1/2$, x, $-z+1/2$; ^{iii} y, $-x+1/2$, $-z+1/2$ for **4**.

2 Results and discussion

2.1 Structure description of 1

Single crystal X-ray diffraction analysis reveals that complex **1** crystallizes in the monoclinic space group *Pc*, and the selected bond distances and angles are listed in Table 2. Complex **1** has a mononuclear structure, as shown in Fig.1. The structural unit of **1** contains an independent Mn(Ⅱ) cation, four neutral L^1 ligands and two OH^- anions. The Mn(Ⅱ) center is six coordinated to complete a distorted octahedral geometry. The equatorial plane is formed by four N atoms from four distinct L^1 ligands and the axial position are occupied by two O atoms from two OH^- anions. The coordination angles around Mn(Ⅱ) center are vary from 86.2(3)° to 179.1(3)°. The Mn-O bond lengths are 0.214 9(5) nm and 0.216 5(5) nm, respectively. The lengths of Mn-N bonds are 0.222 8(7), 0.225 3(6), 0.225 4(7) and 0.226 3(7) nm, respectively. The L^1 acts as a monodentate ligand in complex **1** and two-coordinated OH^- anions not only participated in coordination but also acts as a counter anion for charge balance.

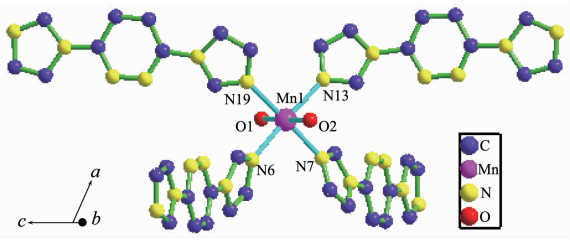

Fig.1　View of the coordination environment of Mn(Ⅱ) ion in **1**

2.2 Structure description of 2

Complex **2** crystallizes in the tetragonal space group $P4_12_12$. Crystallographic data and experimental details for structural analyses were summarized in Table 1. In **2**, each Mn(Ⅱ) center adopts a slightly distorted octahedral coordinated by two N atoms from two L^1 ligands (Fig.2) and four O atoms from water molecules. The N1^{i}-Mn1-N6 coordination angle is 98.6(2)°. The Mn-N bond distances are 0.226 1(5) and

0.226 2(5) nm, respectively. (see Table 2). The Mn-O bond distances are 0.216 5(5), 0.218 4(5), 0.219 9(5), and 0.222(5) nm (see Table 2), respectively. The two imidazole rings are coplanar with the central pyridazine ring. The L^1 ligands, acting as a bisconnector, link Mn(Ⅱ) centers to form the 1D chain with the Mn…Mn distance of 1.311 9 nm. From such coordination mode, the $[MnL^1(H_2O)_4]^{2+}$ unit has two positive charges. The SO_4^{2-} anions don′t show any bonding interaction with Mn(Ⅱ) centers, and only acts as a counteranion for charge balance.

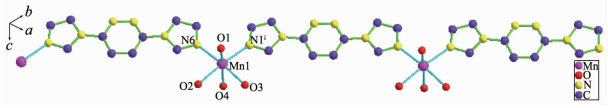

H atoms are omitted for clarity; Symmetry codes: ⁱ $x-1, y-1, z$

Fig.2 View of 1D chain structure of **2**

2.3 Structure description of 3

Complex **3** crystallizes in the monoclinic space group $P2_1/c$ and displays 2D network structure, as shown in Fig.3. The structure unit of **3** contains one Cd(Ⅱ) ion, two L^2 ligands and three coordinated NO_3^- anions. As shown in Fig.3a, The Cd(Ⅱ) ion is seven-coordinated to two N atoms from two distinct L^2 ligands (the Cd-N lengths are 0.225 2(4) and 0.226 3(4) nm, respectively) and five O atoms from distinct three nitrate anions (the bond lengths of Cd1-O1, Cd1-O2ⁱⁱ, Cd1-O3, Cd1-O4 and Cd1-O6 are 0.271 4(3), 0.244 6(3), 0.235 9(3), 0.230 8(4) and 0.282 5(5) nm, respectively). Each Cd(Ⅱ) ion demonstrates a distorted monocapped octahedral geometry. The combination of Cd(Ⅱ) centers

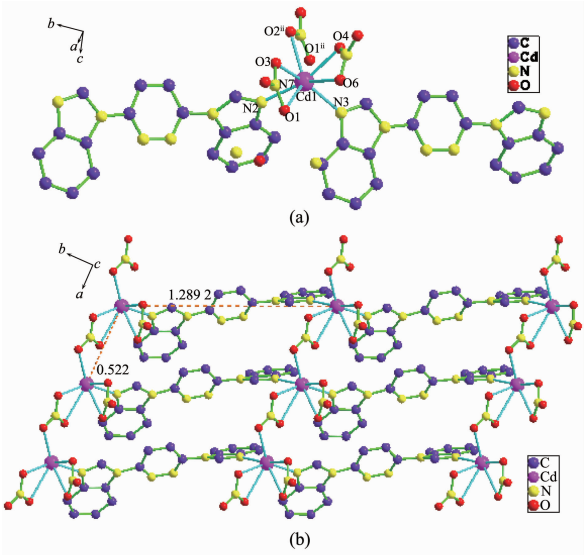

H atoms are omitted for clarity; Symmetry codes: ⁱⁱ $-y+1/2, x, -z+1/2$

Fig.3 View of the coordination environment of Cd(Ⅱ) ion in **3** (a) and the 2D net of the complex **3** (b)

and rigid ligands L^1 form an infinite 1D chain, and the 1D chains are further assembled into a 2D network structure through NO_3^- anions bridging coordination mode, as shown in Fig.3b. The bond angles around Cd(Ⅱ) center vary from 49.95(10)° to 163.18(14)°. The neighboring non-bonding Cd…Cd distance connected by L^2 is 1.289 2 nm, and Cd…Cd distance connected by NO_3^- anion is 0.522 0 nm.

2.4 Structure description of 4

Complex **4** crystallizes in the tetragonal with space group $P4_2/n$. The structural unit of **4** contains a Co(Ⅱ) ion, four neutral L^2 ligands, two uncoordinated PF_6^-. The $Co^{Ⅱ}$ center is coordinated to four N atoms

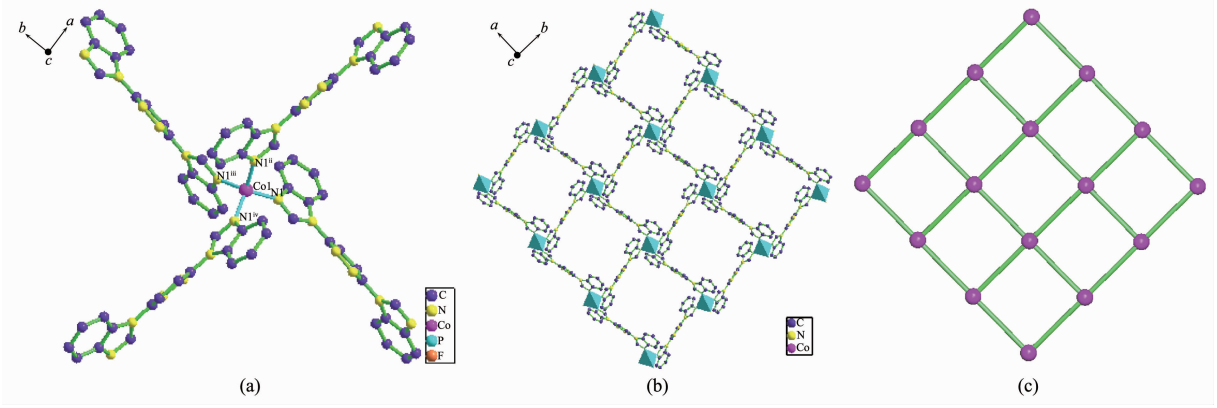

H atoms are omitted for clarity; Symmetry codes: ⁱⁱ $-y+1/2, x, -z+1/2$; ⁱⁱⁱ $y, -x+1/2, -z+1/2$; ⁱᵛ $x+1/2, -y+1/2, z$

Fig.4 View of the coordination environment of Co(Ⅱ) ion in **4** (a), 2D network structure of **4** (b) and the 4^4 topology of **4** (c)

from four distinct L^2 ligands (the Co-N bond lengths are 0.199 6(5) nm) to complete a distorted tetrahedral coordinated geometry with the coordination angles around Co(Ⅱ) center being 107.84(14)° and 112.8(3)°, respectively (Fig.4a and Table 2). Each L^2 ligand links two Co(Ⅱ) centers and in turn each Co(Ⅱ) center connects four ligands forming a layer structure with (4, 4) foursquare grid units. Meanwhile, and all the Co(Ⅱ) centers are located in one plane (Fig.4c). As shown in Fig.4b, each (4, 4) grid unit is constructed by four ligands acting as four edges and four Co(Ⅱ) centers as four vertexs. All the lengths of the edges are equal (the edges are 1.264 5 nm) and the orthogonal distance is 1.788 3 nm. The uncoordinated PF_6^- anions locate at the cavities of the sheets to serve as counter anions.

2.5 Thermogravimetric analysis

To examine the thermal stabilities of complexes **1**~**4**, the TGA analyses of complexes were carried out at the rate of 10 ℃·min^{-1} in nitrogen atmosphere (**1** and **2**: from room temperature to 1 000 ℃; **3** and **4**: from room temperature to 700 ℃) as shown in Fig.5. The TGA study of complex **1** shows a slow weight loss from 30 to 270 ℃, Then the weight loss occurred continuously within the range of 270~1 000 ℃. The TGA curve of **2** displays a weight loss of 20.76% (Calcd. 16.54%) in the range of 100 ~164 ℃ corresponding to the loss of four coordinated water molecule. Above 164 ℃, a rapid weight loss is observed which can be attributed to the decomposing of the organic ligands. The remainder may be MnO_2 (Obsd. 23.38%, Calcd. 19.97%). Complexes **3** and **4** lose weight in the range of 315~620 ℃ and 332~590 ℃, respectively, corresponding to the decomposition of ligands and the remains are CdO for **3** (Obsd. 22.08%, Calcd. 23.39%), CoO for **4** (Obsd. 9.22%, Calcd. 7.69%).

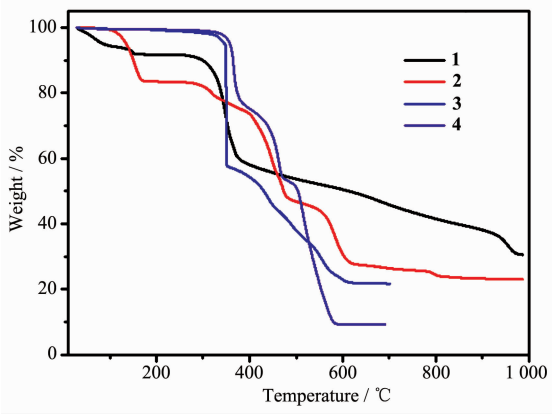

Fig.5 TGA curves of complexes **1**~**4**

2.6 XRPD patterns

To confirm whether the crystal structures are truly representative of the bulk materials, X-ray powder diffraction (XRPD) experiments were carried out for complexes **1**~**4**. The XRPD experimental and computer-simulated patterns of the corresponding complexes are shown in Fig.6. Although the

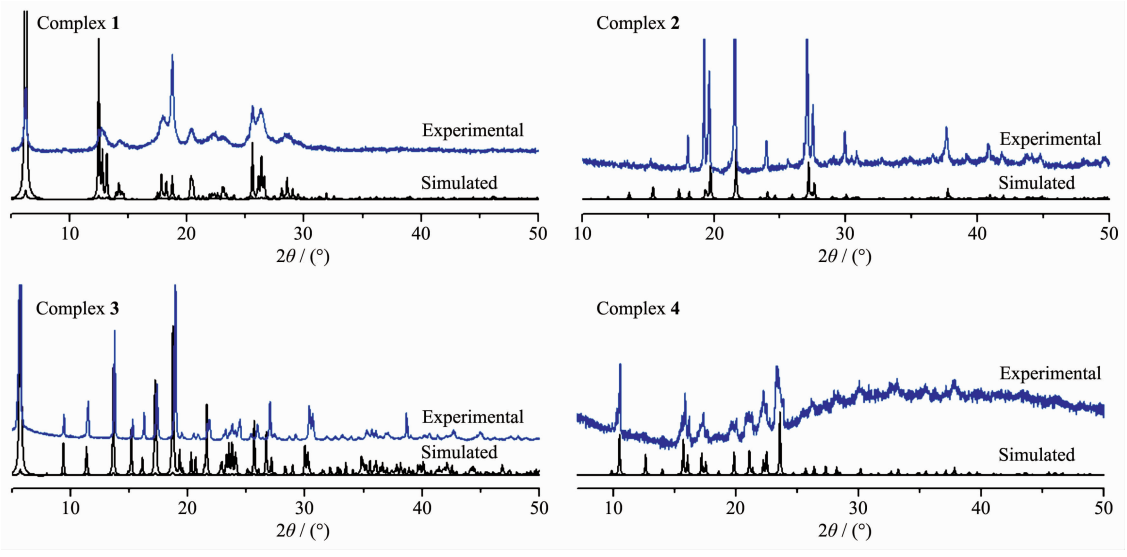

Fig.6 XRPD patterns of **1**~**4**

experimental patterns have a few unindexed diffraction lines and some are slightly broadened in comparison with those simulated from the single crystal modes, it still can be considered favorably that the bulk synthesized materials and the as-grown crystals were homogeneous for **1**~**4**.

2.7 Luminescent properties

Luminescent materials are of great interest due to their various applications in chemical sensor, photochemistry and light-emitting diodes (LEDs). Hence photoluminescence properties of **3**, **4** and ligand L^2 are investigated in the solid state at room temperature, as shown in Fig.7. Upon excitation with 370 nm light, the free ligand L^2 present emission bands at 469 nm. Complexes **3** and **4** all exhibit fluorescent emission with the maxima at 469 and 407 nm, upon excitation at 370 and 250 nm, respectively. The emission of the ligand may be assigned to $\pi^* \rightarrow n$ or $\pi^* \rightarrow \pi$ transitions of the intra-ligands[23]. The emission peak of **3** is similar to the free ligand. It should be pointed out that the emission of complex **3** is neither metal-to-ligand charge transfer (MLCT) nor ligand-to-metal charge transfer (LMCT) in nature since the Cd(Ⅱ) is difficult to oxidize or to reduce due to its d^{10} configuration[13]. Therefore they are mainly based on the intra-ligand transitions. However, the maximum emission wavelength of complex **4** is blue-shifted, which is probably due to intra-ligand charge transitions[24]. The differences of the peaks for **3** and **4** may result from different coordination and conformations[25].

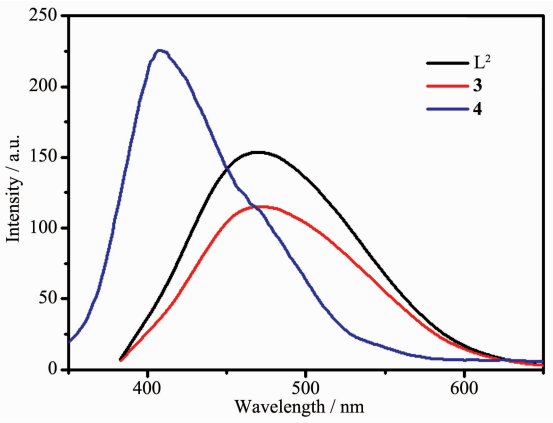

Fig.7 Emission spectra of **3**, **4** and L^2 in the solid state at room temperature

2.8 Photocatalytic activity

Photocatalysts have attracted much attention because of their potential application in purifying water by thoroughly decomposing organic pollutants. In this work, the photocatalytic activities of complexes **3** and **4** were investigated with the photodegradation of MB. The decomposition of MB was monitored by the characteristic absorption band at 664 nm. The final results showed that the degradation rate of MB added the complex **4** and added no complex are almost equal, but the degradation rate of MB is 79% when added complex **3** after 4 h under UV irradiation, as shown in Fig.8. The results showed that **3** is efficient catalysts for MB degradation, however, complex **4** is nearly inefficient catalysts for MB. The different photocatalytic performances of complexes **3** and **4** may be due to their different components and structures[26].

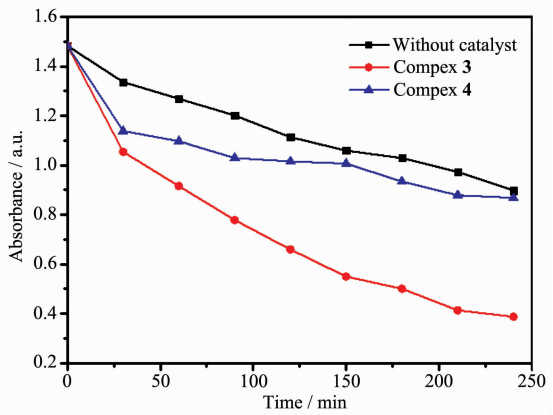

Fig.8 Curves of absorbance of the MB solution degraded by **3**, **4** under UV light

3 Conclusions

In conclusion, we have successfully synthesized and characterized four new complexes based on the ligands 3,6-bis(*N*-imidazolyl) pyridazine (L^1) and 3,6-bis (*N*-benzimidazolyl) pyridazine (L^2). X-ray diffraction analyses reveal that complex **1** has a mononuclear structure and complex **2** features a 1D structure. Complexes **3** and **4** exhibit 2D network structures. Moreover, the fluorescence properties of ligand L^2 and complexes **3** and **4** display blue fluorescent emission at room temperature. The photocatalytic activities of complexes **3** and **4** proved that **3** may be photocatalysts

for degradation of organic dyes in a certain extent.

Supporting information is available at http://www.wjhxxb.cn

References:

[1] Li B, Tian F Y, Qin C, et al. *Russ. J. Coord. Chem.*, **2015**, **41**:706-714

[2] Qin L, Xiao S L, Ma P J, et al. T*ransition Met. Chem.*, **2013**, **38**:627-633

[3] An H Y, Wang L, Hu Y, et al. *CrystEngComm*, **2015**,**17**: 1531-1540

[4] Guo F, Zhu B Y, Liu M L, et al. *CrystEngComm*, **2013**,**15**: 6191-6198

[5] He H M, Song Y, Sun F X, et al. *Cryst. Growth Des.*, **2015**, **15**:2033-2038

[6] Liang G R, Liu Y R, Zhang X, et al. *Synth. React. Inorg. Met.-Org. Chem.*, **2016**,**46**:251-256

[7] Tomono K, Otani E, Ikeda R, et al. *J. Inclusion Phenom. Mol. Recognit. Chem.*, **2011**,**70**:241-247

[8] Li X J, Yu Z J, Guan T, et al. *Cryst. Growth Des.*, **2015**,**15**: 278-290

[9] Li G B, He J R, Pan M, et al. *Dalton Trans.*, **2012**,**41**:4626-4633

[10]Zhang X Y, Zhang Y H, Liu S Z, et al. *Inorg. Chem. Commun.*, **2014**,**46**:289-294

[11]Liu L, Huang C, Zhang L, et al. *Cryst. Growth Des.*, **2015**, **15**:2712-2722

[12]Chen J Q, Cai Y P, Fang H C, et al. *Cryst. Growth Des.*, **2009**,**9**:1605-1613

[13]Chen L, Zhang L, Li S L, et al. *CrystEngComm*, **2013**,**15**: 8214-8221

[14]Li H, Xu G C, Zhang L, et al. *Polyhedron*, **2013**,**55**:209-215

[15]Shao Z C, Huang C, Han X, et al. *Dalton Trans.*, **2015**,**44**: 12832-12838

[16]Wang X L, Sha X T, Liu G C, et al. *CrystEngComm*, **2015**, **17**:7290-7299

[17]Payra P, Hung S C, Kwok W H, et al. *Inorg. Chem.*, **2001**, **40**:4036-4039

[18]Wang X X, Ma Y J, Li H H, et al. *Transition Met. Chem.*, **2015**,**40**:99-108

[19]Li S L, Lan Y Q, Ma J C, et al. *Cryst. Growth Des.*, **2010**, **10**:1161-1170

[20]Chen L, Xu G J, Shao K Z, et al. *CrystEngComm*, **2010**,**12**: 2157-2165

[21]*SAINT Software Reference Manual*, Bruker AXS, Madison, WI, **1998**.

[22](a)Sheldrick G M. *SHELXS* 97, *Program for Solution and Refinemen of Crystal Structures*, University of Göttingen, Germany, **1997**.

(b)Sheldrick G M. *SADABS, Program for Empirical Absorption Correction of Area Detector Data*, University of Göttingen, Germany, **1997**.

[23]Liu K, Ma B H, Guo X L, et al. *CrystEngComm*, **2015**,**17**: 5054-5065

[24]Zhang M D, Qin L, Yang H T, et al. *Cryst. Growth Des.*, **2013**,**13**:1961-1969

[25]Cao L H, Wei Y L, Yang Y, et al. *Cryst. Growth Des.*, **2014**, **14**:1827-1838

[26]Wang X L, Chen N L, Liu G C, et al. *Inorg. Chim. Acta*, **2015**,**432**:128-135